Proceedings of 2021 IEEE
International Conference on Mechatronics and Automation
August 8 - 11, Takamatsu, Japan

Preliminary Evaluation of a Performance-based Stiffness Control for Upper Limb Elbow Joints Rehabilitation

Ziyi Yang[*1], Shuxiang Guo[*2*3], and Yi Liu[*1]

[*1] Graduate School of Engineering
*2 Department of Intelligent Mechanical Systems Engineering
Kagawa University
Hayashi-cho, Takamatsu, 761-0396, Japan

s21d502@kagawa-u.ac.jp

[*3] Key Laboratory of Convergence Medical Engineering System and Healthcare Technology, The Ministry of Industry and Information Technology, School of Life Science
Beijing Institute of Technology
Haidian District, Beijing, 100081, China

guo.shuxiang@ kagawa-u.ac.jp

Abstract –**For post-stroke patient, the interaction force between the impaired limb and the rehabilitation robotic system is an important issue for patient safety in clinical treatment. The compliance control scheme can be achieved by the rehabilitation robotics with variable stiffness actuator (VSA) for the safe physical human robot interaction. The output stiffness would be adjusted independently via variable stiffness actuator during the rehabilitation training processing. In addition, when the stiffness changing, the different impedance characteristic can be realized according to the environmental applied force. The compliance control of VSA can be utilized into the rehabilitation application scenario for improving the training safety. In this paper, a performance-based stiffness control strategy for maximum the rehabilitation effect and increasing the patient participant was proposed utilizing the compliance characteristic of VSA. The elbow joint output stiffness would be regulated according the patient's training performance which will be determined using the real-time position tracking error. It is noted that the training performance should be different to adapt the patient individual-specific. Therefore, an acceptable position tracking error range should be set in advance for the suitable training plan. The experimental results show that the proposed method can adjust the elbow joint stiffness for patients according to the real-time training performance.**

Index Terms – Stiffness Control, Upper limb elbow joint, Performance-based control strategy, Interaction Force, and physical human robot interaction

I. Introduction

Within the aging society processing, the disable people and stroke patients would be rapidly increasing in recent years all over the world [1]. Due to the stroke patients and disable people lack the motor ability and hard to perform the activities of daily living (ADLs). However, the medical resources cannot meet such huge requirement of therapist. Therefore, the robot-assistant system which can assist the patients in daily life and the rehabilitation training has been proposed to offset the huge gap of the medical resources [2]. Compared to the conventional therapy, the rehabilitation robotics can provide the repeatable, intensive predefine therapy to different disability level patients [3]. The rehabilitation robotics are also convinced to adapt the many individual-specific condition by applying different control strategies, which can recurrent the professional recovery training without the therapist.

In the recent years, there are many different kinds of assistant strategy for improving the rehabilitation efficient and speed [4]. it can be mainly divided into two kinds, the biomedical signals-based assistance strategy [5] using EEG, EMG [6] or ECG of the patients and the physical measurement signals-based control strategy utilizing like the contact force [7], motion position angles [8], or motion postures of patients [9]. The biomedical signal-based strategy may increase the difficulty of the high-precision measurement as the dislocation of the biomedical sensors and the patient's skin during the motion perform period. Therefore, the regular physical signals-based strategy was widely used in the rehabilitation robotics researches. In addition, the key parts of the rehabilitation training are the training safety and the training comfortability [10]. The interaction force between the robot and the patient usually be selected as the key factor to evaluate the system comfortability and safety [11]. The force control technology has been wildly introduced in the reference [12]-[13]. Especially for the robotics-assistant rehabilitation system, the safe physical human robot interaction (pHRI) is necessary to be considered during the mechanical design and the system control scheme design. To achieve the safe pHRI, the compliance control strategy is commonly implemented into the rehabilitation systems. The compliance control can be realized by two different methods, the programming compliance, and the passive compliance. The programming compliance means that using the force control of joint driven motors of the robots to softly interact with the environment, which is opposite to the rigid position control. However, the programming compliance required the precision information of the interaction environment. In the rehabilitation application scenario, the weakness of the different patient condition is hard to evaluate and predicted in advance. Therefore, the passive compliance method is a suitable method to solve the above problems. The passive compliance does not mean it cannot be programmed or controlled. The passive compliance refers to the robot have the compliance mechanism, such as the variable-stiffness actuators [14]-[15]. In addition, the rehabilitation training should be

978-1-6654-4098-1/21/$31.00 ©2021 IEEE

designed according to the patient's motor state and patient individual-specific.

In our pervious study, the end-effector type [16] and portable exoskeleton type devices [17] with the variable-stiffness actuator have been proposed for the compliance control. In addition, we also proposed some control methods to achieving the friendly pHRI and efficient assistant training [18]-[23]. For the compliance assistant with VSA, the position tracking evaluation experiments were carried out to validate the deviation angle in the different stiffness [24]. However, the interaction force has not been validated for safe pHRI. In this study, not only the interaction force, but the performance-based stiffness control for increasing the safety and training efficient was proposed. The performance-based stiffness control framework was implemented into a powered variable-stiffness exoskeleton device which has the ability of independently adjust the joint output stiffness by VSA. Furthermore, the acceptable error range was also taken into the control scheme for activating the robot assistant, which can motivate the patient's participation rather than passive training. The appropriate assistant force can be given to the patients only if the training performance is over the error range. This kind of assisted-as-needed (ANN) is beneficial for rehabilitation training as it can maximum the patient active efforts [25].

This paper has been divided into four parts. The section I gives a brief overview of the control strategy with the compliance actuators. Section II begins by laying out the details of system modelling and the performance-based stiffness control method. Section III sets up the experiment, analyses the results gathered and evaluates the effect of the proposed control framework. Section IV draws together the key results and gives our conclusion.

II. Methods

A. Hardware Platform

In this study, the interaction force between the patient and the robot would be evaluated by the powered variable-stiffness exoskeleton device (PVSED). The prototype design of the PVSED was detailed introduced in the previous research [26]. The PVSED is different from the normal exoskeleton device because the variable-stiffness actuator of PVSED was middle part between the transmission mechanism and the output link which can allow the compliance mechanical properties. The physical prototype of the PVSED is shown as the Fig. 1. As the Fig. 1 shows, the PVSED can be easily carried on the patients' back with the shoulder straps and belts which is portable and convince for the home-based rehabilitation scenarios. In order to reducing the weight burden of patients, the light-weight aluminum alloys were selected as the main exoskeleton frames materials and the Acrylonitrile Butadiene Styrene (ABS) was selected for the shoulder connection part materials. The total weight of the PVSED is 3.1kg and the weight load can be distributed to the shoulder and torsos via the two symmetry shoulder straps and a torso belt to improve comfortability and wearability of the device. In order to adapt individual-specific, the adaptive mechanism for different body size was considered

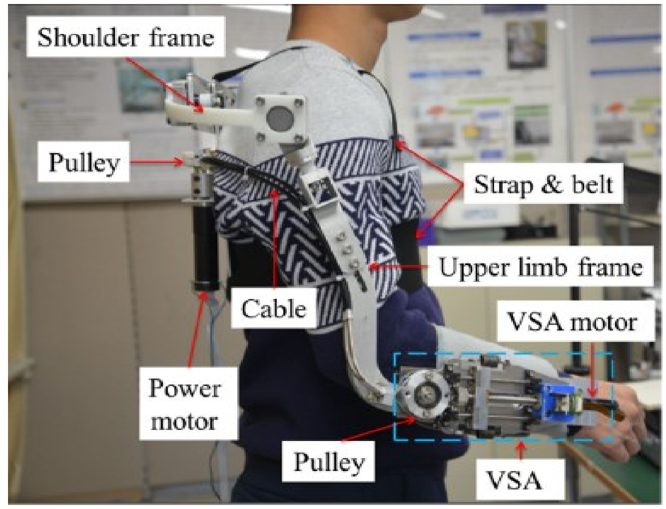

Fig.1. Overall structure design of the PVSED.

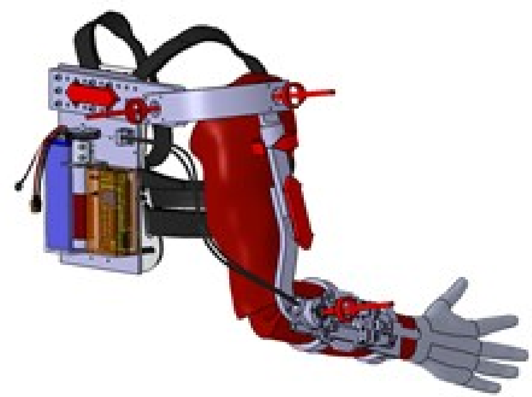

Fig.2. Adaptable structure of the PVSED

which can adjust the length of arm and the wide of shoulder as Fig. 2 shows. Additionally, considering the position of the centre of the glenohumeral joint is changed during the upper limb movements, the three passive shoulder degree of freedoms (DoFs) were designed to reduce the misalignment of the exoskeletal and the human joint axes and allow the nature range of motion of wears. The 3 passive shoulder DoFs includes the shoulder adduction/abduction, shoulder flexion/extension and internal/external rotation, respectively. Therefore, the high wear-comfortability and high adaptability to individual-specific of the PVSED can be achieved for facilitating the rehabilitation effect.

The transmission mechanism of the PVSED has two parts including the elbow motion transmission part and the variable-stiffness transmission part. The elbow motion transmission part is a light-weight cable-driven mechanism which can assist the wears via a compact DC motor (Maxon RE-30 Graphite Brushes Motor) placed on the back frames. One advantage of the cable-driven mechanism is the high back-drivability. The stiffness adjustment mechanism on the forearm which is also called the variable-stiffness actuator (VSA) is independent to the elbow motion transmission mechanism. The VSA is consisted of a small-size DC motor (Maxon RE-13 Graphite Brushes Motor), a screw ball transmission with the pivot, and a pair of antagonistic springs as the Fig. 3. The pivot can be moved by the DC motor through the screw ball transmission to

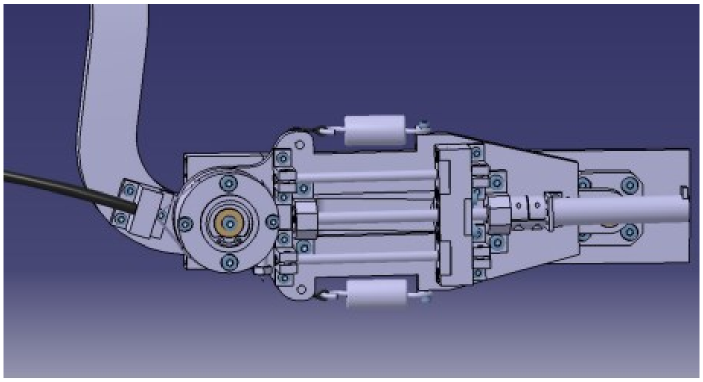
Fig.3. CAD Model of the integrated VSA

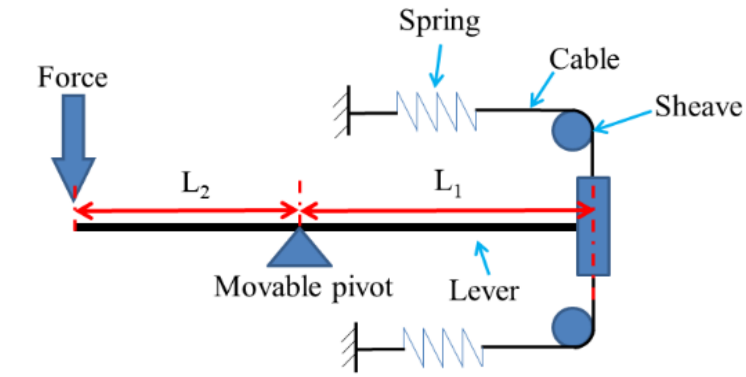

Fig.4. Working princinple of the VSA

regulate the lever ratio of the output link and the antagonistic springs for variable stiffness.

B. Working Principle of Variable-stiffness Actuator

In this part, the working principle would be introduced in detail for the dynamic model. The conceptual model of the VSA is shown as the Fig. 4. The ends of the antagonistic springers were fixed to the main frames and the other ends were fixed to the output link by the steel cables. The pivot was implemented into the ball screw and powered by the DC motor. The transmission ratio of the exerted load and the spring force can be adjusted according to the pivot position changes resulting the stiffness variable characteristic.

$$K = \frac{\tau}{\theta} \tag{1}$$

Where the K is represented the stiffness, the τ is the applied torque and the θ is the angular change to the initial position. The applied torque can be calculated by the applied force F and the level l, so the formula 1 can be written as:

$$K = \frac{F \cdot l}{\theta} \tag{2}$$

As the Fig. 4, the equilibrium of moment can be written as follows:

$$F_{spring} \cdot L_1 = F \cdot L_2 \tag{3}$$

Where the L_1 is the lever of the spring force, and the L_2 is the lever of the applied force. According to the Hooke's Law:

$$F_{spring} = k \cdot x_d \tag{4}$$

Where the x_d is the elongation of the spring. For the PVSED, the elasticity coefficient of spring is set as 19.6 N/mm.

$$K = \frac{F_{spring} \cdot l}{\theta_d} \cdot \frac{L_1}{L_2} \tag{5}$$

The L_1/L_2 represents the transmission ratio which is the position of the pivot. The relationship between the output stiffness and the pivot position can be described by a 2 order polynomial fitting as follows:

$$K = 0.1443 \cdot d^2 + 2.287 \cdot d + 16.95 \quad (0mm \leq d \leq 20mm) \tag{6}$$

Due to the motor 2 is controlled by a position controller, the pivot position can be easily calculated by the parameter of the ball screw and the rotation of the motor 2. Therefore, the output force can be actively regulated by controlling the pivot position.

C. Dynamics model of PVSED

The 1-DOF joint with independent-driven variable-stiffness actuator [27] can be modeled as the compliance joint with a elasticity parameter. Motivated by the [28], the whole system modeling (shown as Fig. 5) of the 1-DOF elbow joint exoskeleton with the VSA can be described as follows:

$$J_m\ddot{\theta}_j + B_m\dot{\theta}_j + G(\theta_j) = \tau_j + \tau_{ext} \tag{7}$$

$$J_1\ddot{\theta}_1 + B_1\dot{\theta}_1 + \tau_j = \tau_1 + \tau_{ext,1} \tag{8}$$

$$J_2\ddot{\theta}_1 + B_2\dot{\theta}_1 + \tau_s = \tau_2 + \tau_{ext,2} \tag{9}$$

$$\tau_j = K(\theta_2) \cdot (\theta_j - \theta_1) \tag{10}$$

where the J_m is the moment of inertia of the output link of the joint. The J_1 and J_2 are the moment of inertia of the motor rotor, M_1 and M_2, respectively. The B_m is the damping coefficient of the output link, and the B_1 and B_2 are the damping coefficient of the motor rotor, M_1 and M_2. The τ_j represent the output torque of the joint. The τ_{ext} is the applied force on the output link. As the affect of output torque and the applied force, the resistance torque on the motor 1 and the motor 2 can be approximate as the $\tau_j, \tau_{ext,1}, \tau_s$, and $\tau_{ext,2}$.

As the rehabilitation application scenario, the elbow joint motion can be performed in a relatively low velocity, which means the angular velocity and the angular acceleration velocity can be approximate as zero. Therefore, the whole system modelling can be simplified as

$$G(\theta_j) = \tau_j + \tau_{ext} \tag{11}$$

The gravity of the output link can be written as

$$G(\theta_j) = m \cdot g \cdot l \cdot \sin(\theta_j) \tag{12}$$

Substituting the formula 12 into formula 11, the simplification modelling of the 1-DOF elbow joint with VSA is given:

$$m \cdot g \cdot l \cdot \sin(\theta_j) = K(\theta_2) \cdot (\theta_j - \theta_1) + \tau_{ext} \tag{13}$$

From the furmula 13, the function of the desried stiffness can be calculated when the system was applied a interaction force which leads to the deviation angle between the main frame and the output link.

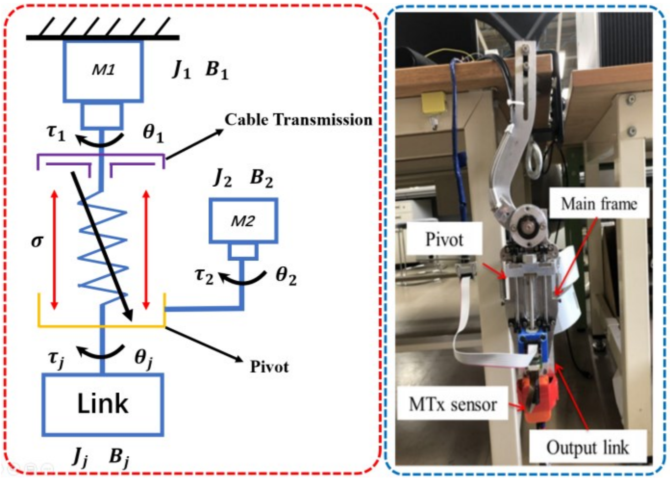

Fig.5. Dynamic modeling of the PVSED

D. Performance-based Stiffness Control strategy

In the rehabilitation training processing, the huge motion tracking error would lead the low efficient, which reduced the long training term and would have the potential of motor injury during training processing. In order to improve the efficient of rehabilitation training and let patient to sense the limb motor error, the performance-based stiffness control strategy has been proposed in this study through the VSA-based real-time stiffness adjustment. The performance evaluation method is mainly considered as the position accuracy which can be described as the $\theta_j - \theta_1$. Due to the safety considering and the maximise the patient participant, an acceptable position error range should be considered. Only if the position error over the set error range bound, the performance-based stiffness control strategy would be activated for training effect improvement. In the PVSED, two inertial measurement unit (MPU-6050) are implemented on the output link and main frame respectively to record the θ_j and θ_1. In addition, the patient safety and comfortability are the other key point of rehabilitation training. For improving the patient safety, a thin film piezoelectric sensor (FSR-402) is integrated into the forearm holder against to the patient's injured forearm for real-time force monitoring.

The performance-based stiffness control is based on the simplification modelling of the PVSED. The position deviation and the applied force would be collected in real-time feedback signals to calculate the desired stiffness. There is inner stiffness control loop with a PID controller to calculate desired pivot position and the desired angle of motor 2 for achieving the real-time stiffness regulation. In the out loop, according to the stiffness changes, the deviation angle between the output link and the main frame could be reduced to improve the rehabilitation effect. In the out loop, a PID controller is implemented for the quick position control.

III. EXPERIMENTS AND RESULTS

A. Interaction Force Evaluation Experiments

As the compliance character of the VSA, the position tracking error between the patient limb which also referring to the output link and the main frame of PVSED will bring the

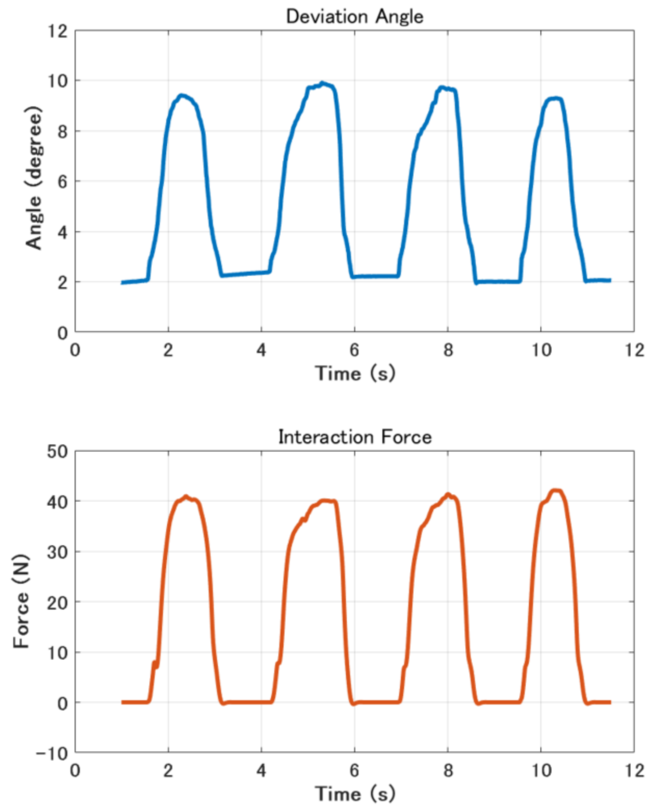

Fig.7. Interaction force evaluation results in Low-stiffness condition

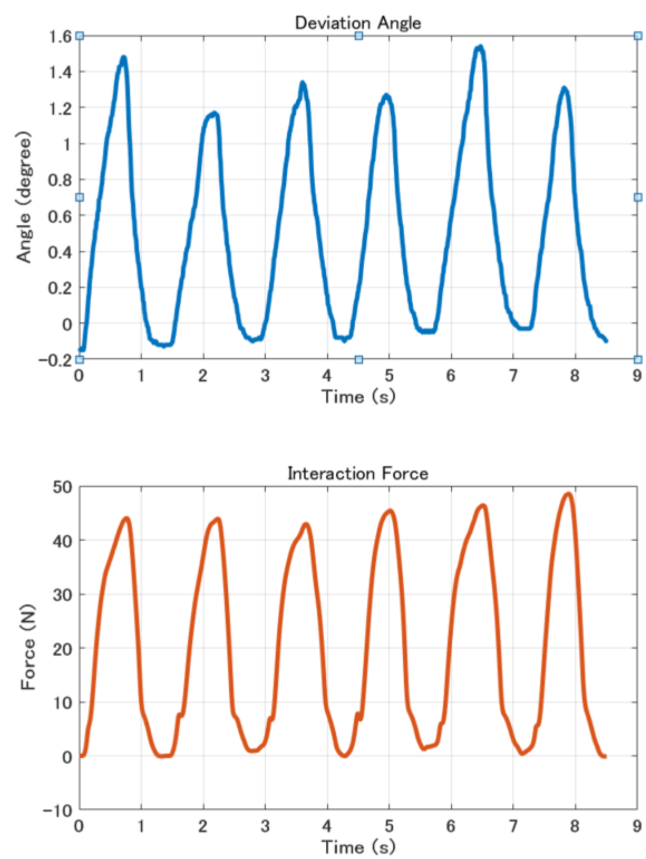

Fig.8. Interaction force evaluation results in Middle-stiffness condition

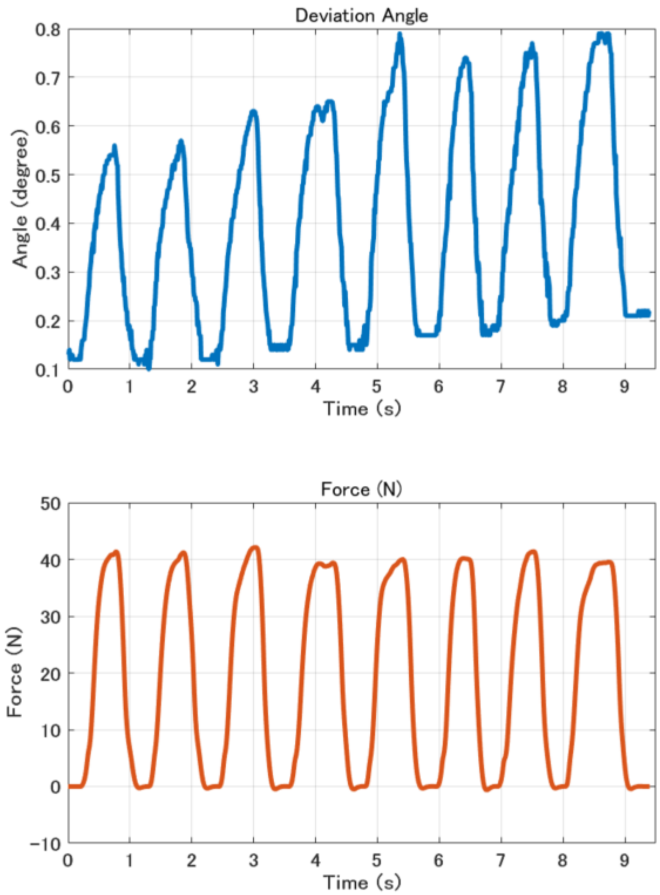

Fig.9. Interaction force evaluation results in High-stiffness condition

interaction force to the patients. This compliance interaction should be evaluated for the comfortable physical human robot interaction and the safety of patients. To validate the interaction performance of the PVSED, the interaction force evaluation experiment would be carried out at first. In the PVSED, two inertial measurement unit (MPU-6050) are implemented on the output link and main frame respectively to record the θ_j and θ_1. And a thin film interaction force sensor was placed on the forearm holder for the comfortable wearability. The experiment protocol is set that the identical force would be applied to the forearm holder sensor part in the different stiffness statement. The position tracking results, which is the deviation of the output link and the main frame, and the interaction force results would be collected in the real-time by the compact control unit (Arduino Mega 2560). The interaction force evaluation experiments were carried out at the pivot position 0mm, 10mm, and 20mm, respectively referring to the low stiffness condition, middle stiffness condition and high stiffness condition.

The interaction force evaluation experimental results were shown as the Fig. 7. In the low-stiffness condition as the Fig. 7, the max value of deviation angles are 9.6 degrees according to the interaction force at 40N. In the middle-stiffness as the Fig. 8, the max value of the deviation angles are 1.5 degrees at the same interaction force 40N. In the high-stiffness as the Fig. 9, the max value of the deviation angles are 0.8 degrees at the

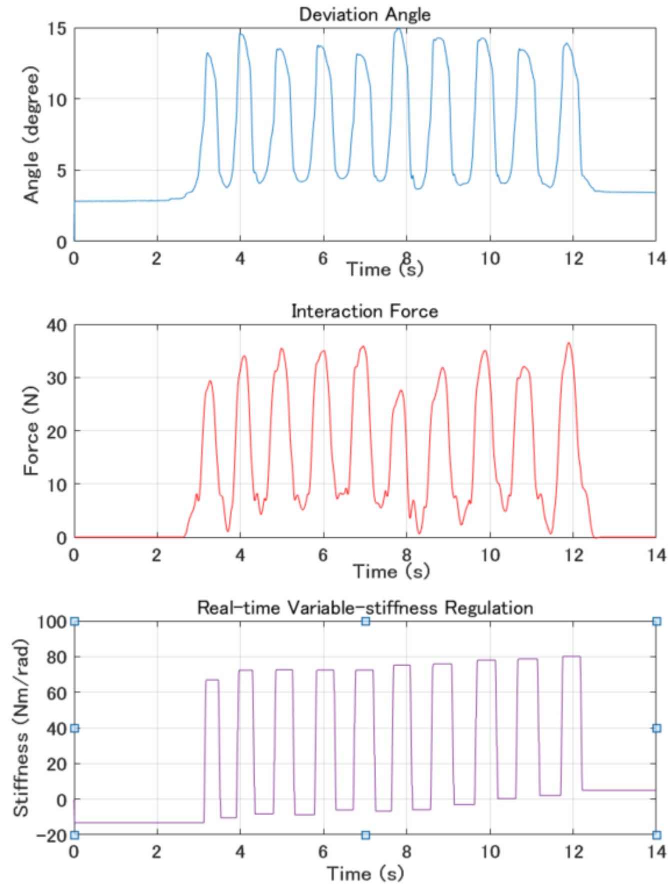

Fig.10. Interaction force evaluation results in Low-stiffness condition

same interaction force 40N. From the above experimental results, we can know that the variable stiffness condition would perform the different impedance characteristics. The high-stiffness condition will have the lowest deviation range which means that the high interaction force can be delivered to the patients for high precision tracking training. The low-stiffness condition can allow patients to perform their own motion with high acceptance. The different stiffness conditions have the special application scenario according to the patient's injury situation during the rehabilitation processing. It is noted that the initial position in the high-stiffness condition was not back to the zero position. The reason of this problem is that the cable-driven transmission has high back-drivable and the cable tension is not tight enough.

B. Performance-based Stiffness Control Experimental Results

To felicitate the rehabilitation training effect, the performance-based training was proposed for achieving the high precision tracking effect. When the patients can not finish the predefine tracking, the assistant force would be applied to the patient's arm through the exoskeleton device. As the mentioned before, the assistant force will be achieved by the VSA by setting an acceptable error range. In this study, the performance-based stiffness control was proposed. In order to evaluate the performance of the performance-based stiffness control, a preliminary evaluation experiment was carried out within the interaction force evaluation experimental frameworks. The performance-based stiffness control experimental results were shown as the Fig. 10. The stiffness can be adjusted when the deviation angle exceeds the set range. The max stiffness was controlled at the 80 Nm/rad according to the deviation angle. When the interaction force reducing to the zero, the deviation angle would be offset by the resistant force of VSA. The stiffness would be controlled to the initial position at the real-time. Same to the interaction force evaluation experiment, the preload and tension of the cable-driven transmission may lead to the initial position error during the rehabilitation training processing.

IV. CONCLUSIONS

In this paper, we proposed a performance-based control strategy which is applied on a powered variable-stiffness exoskeleton device for safe home-based rehabilitation training. Firstly, the interaction force evaluation of the VSA is validated in different stiffness condition. The experimental results show that with the increase of joint stiffness, the lower deviation angle would reduce at the same interaction force level. Further, a preliminary performance-based stiffness adjustment experiment was performed to evaluate the assistant force strategy. The results show that the output stiffness could be regulated when the deviation angle over the deviation angle range for correcting the tracking errors. By the aid of the proposed performance-based stiffness control method, the powered variable-stiffness exoskeleton device has the potential to help the patients complete homebased self-rehabilitation training in different intension.

REFERENCES

[1] E. J. Benjamin *et al.*, "Heart Disease and Stroke Statistics-2019 Update: A Report From the American Heart Association," *Circulation*, vol. 139, no. 10, pp. 56–528, doi: 10.1161/CIR.0000000000000659, 2019.

[2] G. Bao, L. Pan, H. Fang, X. Wu, and H. Yu, "Academic Review and Perspectives on Robotic Exoskeletons," *IEEE Trans. Neural Syst. Rehabil. Eng.*, vol. 27, no. November, pp. 2294–2304, doi: 10.1109/TNSRE.2019.2944655, 2019.

[3] H. I. Krebs, "Twenty + years of robotics for upper-extremity rehabilitation following a stroke. " *Elsevier Ltd.*, pp.175-192, 2018.

[4] M. Babaiasl, S. H. Mahdioun, P. Jaryani, and M. Yazdani, "A review of technological and clinical aspects of robot-aided rehabilitation of upper-extremity after stroke," *Disabil. Rehabil. Assist. Technol.*, vol. 11, no. 4, pp. 263–280, doi: 10.3109/17483107.2014.1002539, 2016.

[5] Z. Yang, S. Guo, Y. Liu, H. Hirata, and T. Tamiya, "An intention-based online bilateral training system for upper limb motor rehabilitation," *Microsyst. Technol.*, vol. 0123456789, doi: 10.1007/s00542-020-04939-x, 2020.

[6] B. Rodríguez-tapia, I. Soto, N. C. Arballo, and D. M. Martínez, "Myoelectric Interfaces and Related Applications : Current State of EMG Signal Processing — A Systematic Review," *IEEE Acess*, vol. 8, pp. 7792-7805, 2020.

[7] E. Abdi, D. Kulic, and E. Croft, "Haptics in Teleoperated Medical Interventions: Force Measurement, Haptic Interfaces and Their Influence on User's Performance," *IEEE Trans. Biomed. Eng.*, vol. 67, no. 12, pp. 3438–3451, doi: 10.1109/TBME.2020.2987603, 2020.

[8] Z. Song, S. Guo, N. Xiao, B. Gao, and L. Shi, "Implementation of human-machine synchronization control for active rehabilitation using an inertia sensor," *Sensors*, vol. 12, no. 12, pp. 16046–16059, doi: 10.3390/s121216046, 2012.

[9] A. Rudenko, L. Palmieri, M. Herman, K. M. Kitani, D. M. Gavrila, and K. O. Arras, "Human motion trajectory prediction : a survey", *The International Journal of Robotics Research*, vol.8, pp.895-935 2020.

[10] J. Bessler, G. B. Prange-lasonder, L. Schaake, and J. F. Saenz, "Safety Assessment of Rehabilitation Robots : A Review Identifying Safety Skills and Current Knowledge Gaps," vol. 8, no. March, pp. 1–18, 2021, doi: 10.3389/frobt.2021.602878, 2021.

[11] J. Bessler, G. B. Prange-lasonder, L. Schaake, and J. F. Saenz, "Safety Assessment of Rehabilitation Robots : A Review Identifying Safety Skills and Current Knowledge Gaps," vol. 8, no. March, pp. 1–18, 2021, doi: 10.3389/frobt.2021.602878, 2021.

[12] D. Xiong, D. Zhang, X. Zhao, and Y. Zhao, "Deep Learning for EMG-based Human-Machine Interaction : A Review," *IEEE/CAA Journal of Automatica Sinica*, vol.8, pp. 512-533, doi: 10.1109/JAS.2021.1003865, 2021.

[13] H. Van Der Kooij, "Admittance control for physical human – robot interaction," *The International Journal of Robotics Research*, vol.37, pp. 1421-1444, doi: 10.1177/0278364918768950, 2018.

[14] S. Li, J. Li, G. Tian, and H. Shang, "Variable stiffness control for SEAs in rehabilitation training," *Adv. Robot.*, vol. 33, no. 7–8, pp. 424–438, 2019, doi: 10.1080/01691864.2019.1602894, 2019

[15] S. S. Jujjavarapu, A. H. Memar, M. A. Karami, and E. T. Esfahani, "Variable stiffness mechanism for suppressing unintended forces in physical human-robot interaction," *J. Mech. Robot.*, vol. 11, no. 2, pp. 1–12, 2019, doi: 10.1115/1.4042295, 2019.

[16] S. Zhang *et al.*, "Integrating Compliant Actuator and Torque Limiter Mechanism for Safe Home-Based Upper-Limb Rehabilitation Device Design," *J. Med. Biol. Eng.*, vol. 37, no. 3, pp. 357–364, 2017, doi: 10.1007/s40846-017-0228-2, 2017.

[17] Y. Liu, Shuxiang Guo, et.al, "Development of a powered variable-stiffness exoskeleton device ofr elbow rehabilitation," *Biomedical Microdevices,* DOI: 10.1007/s10544-018-0312-6, 2018.

[18] S. Guo, Z. Yang, and Y. Liu, "EMG-based Continuous Prediction of the Upper Limb Elbow Joint Angle Using GRNN," *Proc. 2019 IEEE Int. Conf. Mechatronics Autom. ICMA 2019*, pp. 2168–2173, 2019, doi: 10.1109/ICMA.2019.8816401, 2019.

[19] S. Zhang, Q. Fu, S. Guo, and Y. Fu, "Coordinative motion-based bilateral rehabilitation training system with exoskeleton and haptic devices for biomedical application," *Micromachines*, vol. 10, no. 1, 2018, doi: 10.3390/mi10010008, 2018.

[20] S. Zhang, Q. Fu, S. Guo, and Y. Fu, "A Telepresence system for therapist-in-the-loop training for elbow joint rehabilitation," *Appl. Sci.*, vol. 9, no. 8, 2019, doi: 10.3390/app9081710, 2019.

[21] S. Zhang, Q. Fu, S. Guo, and Y. Fu, "Coordinative Motion-Based Bilateral Rehabilitation Training System with Exoskeleton and Haptic Devices for Biomedical Application," *Micromechines*, doi: 10.3390/mi10010008, 2019.

[22] Z. Yang, S. Guo, and Y. Liu, "Comparison of Isometric Force Estimation Methods for Upper Limb Elbow Joints," *2020 IEEE Int. Conf. Mechatronics Autom. ICMA 2020*, pp. 1558–1563, 2020, doi: 10.1109/ICMA49215.2020.9233869, 2020.

[23] Z. Song *et al.*, "Implementation of resistance training using an upper-limb exoskeleton rehabilitation device for elbow joint," *J. Med. Biol. Eng.*, vol. 34, no. 2, pp. 188–196, 2014, doi: 10.5405/jmbe.1337.

[24] Y. Liu, S. Guo, and Z. Yang, "Performance Evaluation of a Powered Variable-stiffness Exoskeleton Device for Bilateral Training," *Proc. 2019 IEEE Int. Conf. Mechatronics Autom. ICMA 2019*, pp. 2163–2167, 2019, doi: 10.1109/ICMA.2019.8816633, 2019.

[25] H. J. Asl, M. Yamashita, T. Narikiyo, and M. Kawanishi, "Field-Based Assist-As-Needed Control Schemes for Rehabilitation Robots," *IEEE/ASME Transactions on Mechantronics*, vol. 4435, no. c, 2020, doi: 10.1109/TMECH.2020.2992090, 2020.

[26] Y. Liu, S. Guo, Z. Yang, H. Hirata, and T. Tamiya, "A Home-based Bilateral Rehabilitation System with sEMG-based Real-time Variable Stiffness," *IEEE J. Biomed. Heal. Informatics*, no. c, pp. 1–1, 2020, doi: 10.1109/jbhi.2020.3027303.

[27] L. Liu, B. J. E. Misgeld, A. Pomprapa, and S. Leonhardt, "A Testable Robust Stability Framework for the Variable Impedance Control of 1-DOF Exoskeleton With Variable Stiffness Actuator," *IEEE Trans. Control Syst. Technol.*, no. January, 2021, doi: 10.1109/TCST.2021.3051716.

[28] L. Liu, S. Leonhardt, C. Ngo, and B. J. E. Misgeld, "Impedance-Controlled Variable Stiffness Actuator for Lower Limb Robot Applications," *IEEE Trans. Autom. Sci. Eng.*, vol. 17, no. 2, pp. 991–1004, 2020, doi: 10.1109/tase.2019.2954769.